KEYNOTE
PERKIN 2

Hammett correlations 'beyond the molecule'[1]

Peter R. Ashton,[a] Matthew C. T. Fyfe,[a] Sarah K. Hickingbottom,[a] J. Fraser Stoddart,*,†,[a] Andrew J. P. White[b] and David J. Williams*,[b]

[a] *School of Chemistry, The University of Birmingham, Edgbaston, Birmingham, UK B15 2TT*
[b] *Department of Chemistry, Imperial College, South Kensington, London, UK SW7 2AY*

The crown ether dibenzo[24]crown-8 (DB24C8) is interpenetrated by a wide range of disubstituted dibenzylammonium cations to generate [2]pseudorotaxane complexes by virtue of, *inter alia*, hydrogen bonds. ^{1}H NMR spectroscopic measurements indicate that the solution phase binding strengths of the pseudorotaxane complexes can be controlled accurately *via* judicious manipulation of the substituents attached to the dibenzylammonium cations' aryl rings. A linear free energy relationship (LFER) has been found to exist between the complexes' stability constants (K_as) and the Hammett substituent constants (σ). X-Ray crystallographic analyses of the pseudorotaxanes reveal that each of their discrete supramolecular units display similar solid state superstructures. However, these analyses also demonstrate that the pseudorotaxanes associate with one another, *via* a myriad of intersupramolecular packing motifs, to generate a wide range of novel superarchitectures.

Introduction

Supramolecular chemistry[2] has evolved rapidly over the past three decades so that the noncovalent syntheses[3] of an extensive[4] range of intricate superarchitectures—held together by means of noncovalent bonding interactions—can now be accomplished with control and precision. Self-assembly[5] has proven to be an especially powerful tool for the construction of these supramolecular edifices, which are often synthesised noncovalently with a particular function in mind. However, before these functions can be realised completely, chemists must first of all grapple with the fundamentals of molecular recognition, so that their basic understanding of the intermolecular bonding interactions, that permit the noncovalent synthesis of ever more complex superarchitectures, is suitably augmented. Accordingly, in this Keynote Article, we discuss our studies on supramolecular structure–activity relationships, in relation to pseudorotaxane‡ formation, with a view to expediting some of our goals in supramolecular synthesis.

Thirty years have passed since Pedersen published[6] his seminal paper on the discovery of the crown ethers, which detailed the binding of ammonium (NH_4^+) and alkylammonium (RNH_3^+) ions—in a face-to-face[7] manner—by dibenzo[18]crown-6 (DB18C6). We have recently extended[8] Pedersen's investigations so that the NH_2^+ centres of the sterically more encumbered secondary ($R_2NH_2^+$) ions can be accommodated centrally within the cavities of macrocyclic polyethers to generate multicomponent pseudorotaxane superarchitectures.[9] By way of illustration, the dibenzylammonium ion ($\mathbf{1}^+$) interpenetrates the cavity of the suitably-sized macrocyclic polyether dibenzo[24]crown-8 (DB24C8) to produce (Scheme 1) a 1:1 inclusion complex exhibiting a pseudorotaxane co-conformation§ in solution, in the 'gas phase' and in the solid state, as demonstrated by ^{1}H NMR spectroscopy, mass spectrometry and X-ray crystallography, respectively. The noncovalent synthesis of the $[DB24C8\cdot\mathbf{1}]^+$ superstructure may be attributed to the stabilising noncovalent bonding interactions that arise as a consequence of (1) hydrogen bonds between the oxygen acceptor atoms of the DB24C8 macroring and the hydrogen donor atoms of the cation's NH_2^+ and CH_2 groups, (2) coulombic interactions involving the NH_2^+ centres and DB24C8's ligating atoms, as well as (3) π–π interactions[10] between the aromatic moieties of each of the pseudorotaxane's components. This simple recognition motif has been[11] developed subsequently for the construction of numerous molecular and supramolecular assemblages with varying stoichiometries and co-conformations. Next, we decided to 'fine-tune' these systems, so that we could control, along with their compositions and co-conformations, the binding strengths of the pseudorotaxanes more precisely. As a result, we have studied pseudorotaxane formation (Scheme 1) between DB24C8 and the salts $\mathbf{1}\cdot PF_6$–$\mathbf{13}\cdot PF_6$ in various solvents/phases. The solution phase studies, presented here, demonstrate that a linear free energy relationship[12] (LFER) exists between the stability constants (K_as) for the formation of the pseudorotaxanes $[DB24C8\cdot\mathbf{1}]^+$–$[DB24C8\cdot\mathbf{13}]^+$ and the Hammett[13] substituent constants (σ).[14] Moreover, X-ray crystallographic studies reveal that, while discrete pseudorotaxanes maintain similar co-conformations in the solid state, there are a large number of distinct interpseudorotaxane packing motifs that are associated with these systems.

Results and discussion

Synthesis

The new disubstituted dibenzylammonium hexafluorophosphate salts $\mathbf{2}\cdot PF_6$–$\mathbf{9}\cdot PF_6$ and $\mathbf{12}\cdot PF_6$–$\mathbf{13}\cdot PF_6$ were readily synthesised using (Scheme 2) a simple four-step protocol, which

† *Present address*: Department of Chemistry and Biochemistry, University of California, Los Angeles, 405 Hilgard Avenue, Los Angeles, CA 90095, USA. Tel.: +(310) 206-7078. Fax: +(310) 206-1843. E-Mail: stoddart@chem.ucla.edu

‡ Pseudorotaxanes have been defined (P. R. Ashton, D. Philp, N. Spencer and J. F. Stoddart, *J. Chem. Soc., Chem. Commun.*, 1991, 1677) as the non-interlocked counterparts of rotaxanes (G. Schill, *Catenanes, Rotaxanes and Knots*, Academic, New York, 1971, p. 3), in which one or more thread-like molecules/ions interpenetrate the cavities of one or more macrocyclic species to generate inclusion complexes. As distinct from rotaxanes, these supramolecular complexes are free to dissociate into their independent components as they do not possess bulky stopper groups. Their analogy in the macroscopic world would consist of one or more beads being threaded onto one or more strings (that have no knots at their ends). Pseudorotaxanes are comprised of *n* components, as indicated by the prefix [*n*].

§ The term 'co-conformation' has been employed previously (M. C. T. Fyfe, P. T. Glink, S. Menzer, J. F. Stoddart, A. J. P. White and D. J. Williams, *Angew. Chem., Int. Ed. Engl.*, 1997, **36**, 2068) to characterise the three-dimensional spatial arrangement of the atoms in molecular and supramolecular entities that are comprised of two or more distinct components.

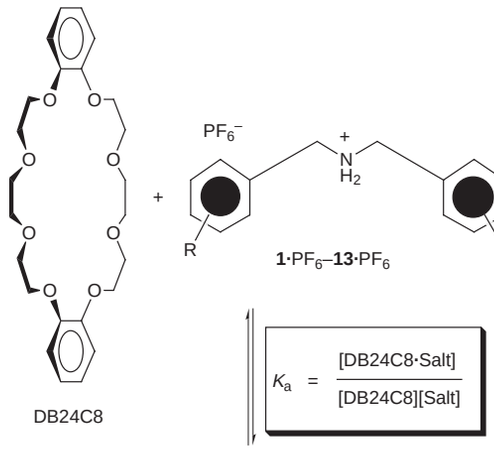

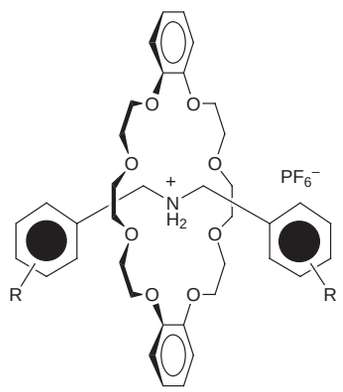

Salt	R	Salt	R
1·PF_6	H	**8**·PF_6	*p*-Br
2·PF_6	*p*-OMe	**9**·PF_6	*m*-Br
3·PF_6	*m*-OMe	**10**·PF_6	*p*-CO_2H
4·PF_6	*p*-Me	**11**·PF_6	*m*-CO_2H
5·PF_6	*m*-Me	**12**·PF_6	*p*-NO_2
6·PF_6	*p*-Cl	**13**·PF_6	*m*-NO_2
7·PF_6	*m*-Cl		

Scheme 1 Dibenzylammonium salts thread their way through the cavity of the DB24C8 macroring to generate [2]pseudorotaxane supermolecules that are stabilised by numerous noncovalent bonding interactions. The pseudorotaxanes' stability constants (K_as) are determined using the relationship K_a = [DB24C8·Salt]/[DB24C8][Salt].

consisted of condensation of the appropriate amine and aldehyde, followed by reduction, acid treatment and counterion exchange.

Solution phase binding studies

The ^{1}H NMR spectra [400.1 MHz, CD_3CN or $CDCl_3$–CD_3CN (1:1), 304 K] of equimolar mixtures of DB24C8 and the dibenzylammonium salts **1**·PF_6–**13**·PF_6 exhibit (Fig. 1) three different sets of resonances (Tables 1 and 2) for (1) free DB24C8, (2) the uncomplexed salt, together with (3) the 1:1 complex formed between both components. This phenomenon has been observed previously[8] for the [DB24C8·**1**]$^+$ complex and indicates that the free and complexed species are equilibrating

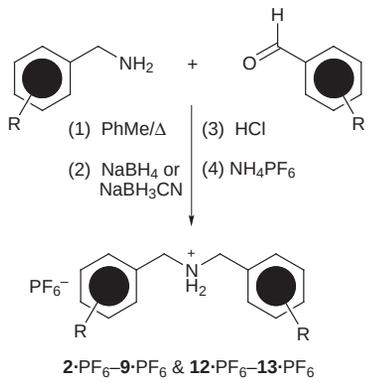

2·PF_6–**9**·PF_6 & **12**·PF_6–**13**·PF_6

Scheme 2 Synthetic procedure employed for the syntheses of the salts **2**·PF_6–**9**·PF_6 and **12**·PF_6–**13**·PF_6

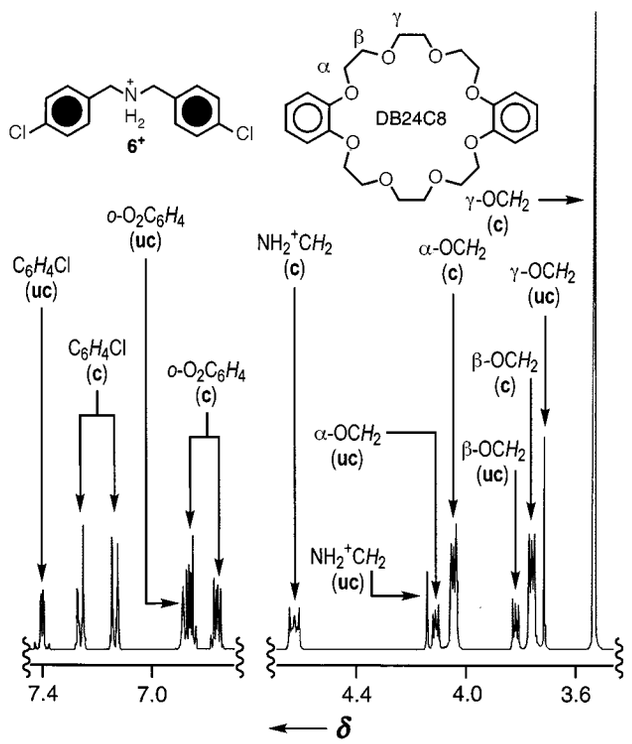

Fig. 1 Representative partial ^{1}H NMR spectrum [400.1 MHz, $CDCl_3$–CD_3CN (1:1), 304 K] of an equimolar solution of DB24C8 and **6**·PF_6 (both 1.0×10^{-2} M), demonstrating that uncomplexed (**uc**) and complexed (**c**) species are equilibrating with one another slowly on the NMR timescale

slowly with one another on the ^{1}H NMR timescale as a consequence of the large steric barrier encountered when the cations' relatively bulky aryl rings attempt to pass through/out of the cavity of the DB24C8 macroring. This kinetic effect permits the calculation of the absolute concentrations of the (1) uncomplexed macrocycle/salt and (2) pseudorotaxane from the known initial crown ether/salt concentrations of the crown ether and the salts and ^{1}H NMR signals' intensities, so that the complexes' K_as, along with their associated free energies of complexation ($-\Delta G°$), may be estimated utilising the so-called single-point[15] method. The K_a values for the complexes [DB24C8·**1**][PF_6]–[DB24C8·**13**][PF_6], in both CD_3CN and $CDCl_3$–CD_3CN (1:1), are displayed in Table 3, in addition to the σ values for the substituents attached to the cations' aromatic rings. Perhaps unsurprisingly, the complexes' solution-phase stability constants are decreased by electron-donating substituents (negative σ values), while they are increased by their electron-withdrawing counterparts (positive σ values). Hammett-type plots[13] were then constructed (Fig. 2) by plotting the log [K_a(R)/K_a(H)] values—where K_a(R) and K_a(H)

Table 1 ^{1}H NMR data[a] (δ values) for the pseudorotaxanes [DB24C8·**1**][PF_6]–[DB24C8·**13**][PF_6] and their uncomplexed constituents (400.1 MHz, CD_3CN, 304 K)[b]

	Crown ether				Dibenzylammonium salt		
Compound/complex	*o*-$O_2C_6H_4$	α-OCH_2[c]	β-OCH_2[c]	γ-OCH_2[c]	$NH_2^+CH_2$	C_6H_4	CH_3
DB24C8	6.89–6.97	4.10	3.80	3.68	—	—	—
1·PF_6	—	—	—	—	4.20	7.44	—
[DB24C8·**1**][PF_6]	6.76–6.88	4.03	3.75	3.51	4.60	7.08–7.15, 7.30	—
2·PF_6	—	—	—	—	4.08	6.92, 7.33	3.79
[DB24C8·**2**][PF_6]	6.75–6.80, 6.82–6.87	4.04	3.75	3.67	4.51	6.64, 7.20	3.50
3·PF_6	—	—	—	—	4.18	6.78–6.94, 7.35–7.39	3.80
[DB24C8·**3**][PF_6]	6.78–6.82, 6.83–6.87	4.06	3.76	3.55	4.66	6.70–6.73, 6.99–7.08	3.61
4·PF_6	—	—	—	—	4.15	7.26, 7.33	2.35
[DB24C8·**4**][PF_6]	6.75–6.81, 6.82–6.88	4.04	3.75	3.57	4.61	6.96, 7.20	2.19
5·PF_6	—	—	—	—	4.14	7.22–7.35	2.35
[DB24C8·**5**][PF_6]	6.82–6.87, 6.88–6.92	4.05	3.75	3.52	4.62	6.99–7.16	2.13
6·PF_6	—	—	—	—	4.15	7.41–7.53	—
[DB24C8·**6**][PF_6]	6.73–6.79, 6.81–6.87	4.03	3.76	3.58	4.65	7.14, 7.31	—
7·PF_6	—	—	—	—	4.19	7.38–7.51	—
[DB24C8·**7**][PF_6]	6.78–6.87	4.06	3.78	3.58	4.67	7.12–7.20, 7.25–7.29	—
8·PF_6	—	—	—	—	4.16	7.37, 7.62	—
[DB24C8·**8**][PF_6]	6.74–6.80, 6.83–6.89	4.03	3.77	3.59	4.65	7.24, 7.30	—
9·PF_6	—	—	—	—	4.17	7.34–7.47, 7.64–7.72	—
[DB24C8·**9**][PF_6]	6.79–6.86	4.06	3.78	3.58	4.65	7.08, 7.28–7.32, 7.57, 7.60	—
10·PF_6	—	—	—	—	4.31	7.56, 8.06	—
[DB24C8·**10**][PF_6]	6.69–6.81	4.01	3.77	3.58	4.78	7.44, 7.75	—
11·PF_6	—	—	—	—	4.31	7.59, 7.69, 8.07, 8.13	—
[DB24C8·**11**][PF_6]	6.71–6.75, 6.76–6.80	4.01	3.78	3.62	4.76	7.25–7.30, 7.59, 7.74–7.78, 8.05	—
12·PF_6	—	—	—	—	4.32	7.72, 8.26	—
[DB24C8·**12**][PF_6]	6.69–6.77	4.02	3.79	3.65	4.88	7.57, 7.96	—
13·PF_6	—	—	—	—	4.34	7.66–7.72, 7.85, 8.35, 8.40	—
[DB24C8·**13**][PF_6]	6.64–6.67, 6.68–6.71	4.00	3.80	3.67	4.88	7.38–7.43, 7.72–7.76, 7.94–7.98, 8.28	—

[a] The spectra were recorded on a Bruker AMX400 Spectrometer employing the peak observed for the residual protons in CD_3CN, at δ 1.93, as the internal reference. [b] The concentrations of the crown ether and dibenzylammonium salt were both 1.0×10^{-2} M initially. [c] The descriptors α, β and γ are defined in Fig. 1.

Table 2 ^{1}H NMR data[a] (δ values) for the pseudorotaxanes [DB24C8·**1**][PF_6]–[DB24C8·**13**][PF_6] and their free constituents (400.1 MHz, $CDCl_3$–CD_3CN (1 : 1), 304 K)[b]

	Crown ether				Dibenzylammonium salt		
Compound/complex	*o*-$O_2C_6H_4$	α-OCH_2[c]	β-OCH_2[c]	γ-OCH_2[c]	$NH_2^+CH_2$	C_6H_4	CH_3
DB24C8	6.86	4.09	3.81	3.70	—	—	—
1·PF_6	—	—	—	—	4.16	7.28–7.31, 7.42	—
[DB24C8·**1**][PF_6]	6.76–6.81, 6.82–6.87	4.05	3.72	3.45	4.62	7.16–7.20	—
2·PF_6	—	—	—	—	4.06	6.92, 7.33	3.79
[DB24C8·**2**][PF_6]	6.77–6.81, 6.83–6.87	4.05	3.74	3.68	4.52	6.66, 7.20	3.51
3·PF_6	—	—	—	—	4.12	7.18–7.32	3.79
[DB24C8·**3**][PF_6]	6.75–6.80, 6.82–6.87	4.05	3.75	3.50	4.61	6.99–7.12	3.60
4·PF_6	—	—	—	—	4.09	7.22, 7.29	2.35
[DB24C8·**4**][PF_6]	6.74–6.79, 6.81–6.86	4.04	3.73	3.50	4.56	6.94, 7.17	2.19
5·PF_6	—	—	—	—	4.10	7.18–7.32	2.35
[DB24C8·**5**][PF_6]	6.77–6.82, 6.84–6.89	4.05	3.73	3.46	4.57	6.98–7.13	2.13
6·PF_6	—	—	—	—	4.13	7.39, 7.41	—
[DB24C8·**6**][PF_6]	6.73–6.77, 6.82–6.86	4.03	3.75	3.54	4.63	7.14, 7.28	—
7·PF_6	—	—	—	—	4.14	7.34–7.44	—
[DB24C8·**7**][PF_6]	6.75–6.80, 6.82–6.88	4.07	3.76	3.52	4.61	7.10–7.22	—
8·PF_6	—	—	—	—	4.12	7.32, 7.57	—
[DB24C8·**8**][PF_6]	6.72–6.78, 6.84–6.90	4.02	3.75	3.53	4.60	7.19, 7.28	—
9·PF_6	—	—	—	—	4.13	7.40–7.44, 7.50–7.65	—
[DB24C8·**9**][PF_6]	6.76–6.81, 6.82–6.87	4.07	3.77	3.52	4.59	7.05–7.10, 7.21–7.26, 7.30–7.36	—
10·PF_6	—	—	—	—	4.26	7.48, 8.08	—
[DB24C8·**10**][PF_6]	6.70–6.75, 6.76–6.81	4.04	3.76	3.55	4.70	7.27, 7.80	—
11·PF_6	—	—	—	—	4.23	7.52, 7.64, 8.04, 8.11	—
[DB24C8·**11**][PF_6]	6.70–6.75, 6.77–6.81	4.03	3.76	3.54	4.68	7.26, 7.45, 7.80, 8.07	—
12·PF_6	—	—	—	—	4.26	7.70, 8.21	—
[DB24C8·**12**][PF_6]	6.66–6.71, 6.74–6.79	4.01	3.78	3.60	4.84	7.52, 7.96	—
13·PF_6	—	—	—	—	4.29	7.48, 7.64, 7.82, 8.35	—
[DB24C8·**13**][PF_6]	6.64–6.69, 6.73–6.78	4.01	3.80	3.65	4.83	7.39, 7.69, 7.95, 8.26	—

[a] The spectra were recorded on a Bruker AMX400 Spectrometer employing the peak observed for the residual protons in CD_3CN, at δ 1.93, as the internal reference. [b] The concentrations of the crown ether and dibenzylammonium salt were both 1.0×10^{-2} M initially. [c] The descriptors α, β and γ are outlined in Fig. 1.

correspond, respectively, to the stability constants for the complexes [DB24C8·**1**][PF_6]–[DB24C8·**13**][PF_6] and [DB24C8·**1**]-[PF_6]—against the σ values. For both solvent systems, a clear straight-line correlation can be observed immediately, suggesting that an LFER exists between the stability constants for the DB24C8–dibenzylammonium salt complexes in solution and

Table 3 Stability constants (K_a) and related free energies of complexation ($-\Delta G°$) for the [2]pseudorotaxane complexes formed between DB24C8 and the disubstituted dibenzylammonium salts **1**·PF_6 –**13**·PF_6[a] in (a) CD_3CN and (b) a $CDCl_3$–CD_3CN (1 : 1) solvent system at 304 K

			CD_3CN			$CDCl_3$–CD_3CN (1 : 1)		
Complex	Substituent (R)	σ[b]	K_a(R)/M^{-1}[c]	log[K_a(R)/K_a(H)][d]	$-\Delta G°$/ kcal mol^{-1}[e]	K_a(R)/ M^{-1}[c]	log[K_a(R)/K_a(H)][d]	$-\Delta G°$/ kcal mol^{-1}[e]
[DB24C8·**2**][PF_6]	*p*-OMe	−0.27	130	−0.19	2.94	990	−0.05	4.17
[DB24C8·**4**][PF_6]	*p*-Me	−0.14	170	−0.07	3.10	960	−0.06	4.15
[DB24C8·**5**][PF_6]	*m*-Me	−0.06	180	−0.05	3.14	1100	0.00	4.23
[DB24C8·**1**][PF_6]	H	0	200	0.00	3.20	1110	0.00	4.24
[DB24C8·**3**][PF_6]	*m*-OMe	0.12	280	0.15	3.40	1350	0.09	4.35
[DB24C8·**6**][PF_6]	*p*-Cl	0.24	470	0.37	3.72	1890	0.23	4.56
[DB24C8·**8**][PF_6]	*p*-Br	0.26	460	0.36	3.70	2010	0.26	4.59
[DB24C8·**11**][PF_6]	*m*-CO_2H	0.35	660	0.52	3.92	2850	0.41	4.84
[DB24C8·**9**][PF_6]	*m*-Br	0.37	570	0.46	3.83	2760	0.40	4.79
[DB24C8·**7**][PF_6]	*m*-Cl	0.37	580	0.46	3.84	2810	0.40	4.80
[DB24C8·**10**][PF_6]	*p*-CO_2H	0.44	510	0.41	3.77	2520	0.36	4.73
[DB24C8·**13**][PF_6]	*m*-NO_2	0.71	1350	0.83	4.35	6460	0.77	5.30
[DB24C8·**12**][PF_6]	*p*-NO_2	0.78	1300	0.81	4.33	5940	0.73	5.25

[a] The initial concentration of both components was 1×10^{-2} M. [b] The Hammett substituent constants (σ) were acquired from O. Exner, *Correlation Analysis in Chemistry*, Plenum, London, 1978. [c] Stability constants (K_a) were obtained as outlined in ref. 8 (percentage error ≤ 15%). [d] The descriptors K_a(R) and K_a(H) denote the stability constants for the formation of the complexes [DB24C8·**1**][PF_6]–[DB24C8·**13**][PF_6] and [DB24C8·**1**][PF_6], respectively. [e] The free energies of complexation ($-\Delta G°$) were calculated from the K_a values using the equation $-\Delta G° = RT \ln K_a$.

the electronic nature of the substituents (as defined[13a,b] by the ionisation of substituted benzoic acids at 298 K, *i.e.* Hammett's original system). This correlation may be ascribed to the influence of the substituents attached to the cations' aromatic rings, since they undoubtedly modify the hydrogen bond donor ability of the NH_2^+ centres and benzylic CH_2 groups, in addition to changing the propensity of the substituted aromatic units to become involved in π–π stacking interactions with the catechol units of the DB24C8 macrocycle. The slopes of the graphs portrayed in Fig. 2 are equivalent to the supramolecular reaction constants (ρ) and have values of +1.03 and +0.86 for the CD_3CN and $CDCl_3$–CD_3CN (1 : 1) solvent systems, respectively. The positive values, similar to those acquired[13a,b] for Hammett's original system, obtained for ρ indicate¶ that the cations' positive charge effectively becomes spread out over the macroring's oxygen atoms upon complexation. Moreover, the fact that Hammett-type correlations are observed‖ with two different solvent systems implies that the cations' aromatic substituents will alter the stability constants of the complexes formed between DB24C8 and the salts **1**·PF_6–**13**·PF_6 regardless of the nature of the solvent present. Nevertheless, the slightly smaller ρ value calculated for the studies carried out in the $CDCl_3$–CD_3CN (1 : 1) solvent system demonstrates that the polar effect exerted by the cations' aromatic substituents has less bearing on pseudorotaxane formation in solvents of reduced polarity. This observation is hardly surprising, inasmuch as these particular pseudorotaxane supermolecules are stabilised[8] to a greater extent in $CDCl_3$ as compared to more polar solvents such as CD_3CN. In other words, the relative importance of the effect that the substituents have on the overall stabilisation of the pseudorotaxanes [DB24C8·**1**][PF_6]–[DB24C8·**13**][PF_6] *decreases* as the solvent's polarity *decreases*.

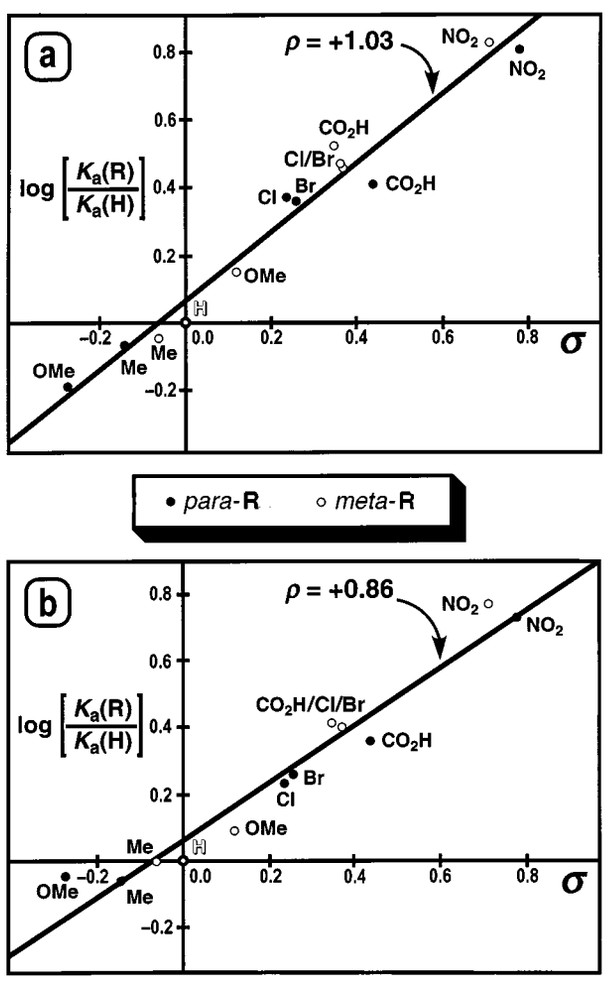

Fig. 2 Hammett correlations between log [K_a(R)/K_a(H)] and σ in (a) CD_3CN and (b) $CDCl_3$–CD_3CN (1 : 1) at 304 K. The slopes of the straight lines obtained correspond to the supramolecular reaction constants (ρ)

X-Ray crystallography

The solid state structures of 11 of the 12 substituted [2]pseudo-

¶ This assertion can be made since the ρ value may be regarded as a measure of the change in the charge density at the (supramolecular) reaction centre, which is, in this instance, the NH_2^+ centre. A positive ρ value indicates (P. Sykes, *A Guidebook to Mechanism in Organic Chemistry*, Longman, Harlow, 6th edn., 1986, p. 368) the effective disappearance of the positive charge at this centre.

‖ The formation of all of the complexes was demonstrated additionally in the 'gas phase' by liquid secondary ion (LSI) mass spectrometry. All of the LSI mass spectra displayed strong peaks for the 1 : 1 complexes with the loss of their PF_6^- anions, *i.e.* [DB24C8·**1**]$^+$–[DB24C8·**13**]$^+$. However, when these mass peaks were calibrated against peaks associated with the bis(4-*tert*-butylbenzyl)ammonium ion—a cation that does not (P. R. Ashton, I. Baxter, M. C. T. Fyfe, F. M. Raymo, N. Spencer, J. F. Stoddart, A. J. P. White and D. J. Williams, *J. Am. Chem. Soc.*, 1998, **120**, 2297) complex with DB24C8—there appeared to be no clear relationship between their relative intensities and the K_a values obtained in solution. In other words, we could not find any evidence for a Hammett correlation in the 'gas phase'.

Table 4 Intrapseudorotaxane hydrogen bonding and π–π interactions[a]

	[N$^+$ ··· O]/Å	[H ··· O]/Å	[N$^+$–H ··· O]/°	[C ··· O]/Å	[H ··· O]/Å	[C–H ··· O]/°	[**A** ··· **C**] interplanar/Å	[**A** ··· **C**]/Å	**A**/**C** tilt/°	[**B** ··· **D**]/Å
[DB24C8·**1**][PF$_6$][b]	2.99, O(2)	2.14	157	3.27, C_D ··· O(7)	2.45	143	3.48	3.79	11	6.74
	3.12, O(8)	2.28	155							
[DB24C8·**2**][PF$_6$]	3.05, O(2)	2.18	161	3.24, C_D ··· O(7)	2.49	134	3.55	3.82	9	6.16
	3.17, O(8)	2.28	170							
[DB24C8·**3**][PF$_6$]	3.11, O(2)	2.28	153	3.29, C_D ··· O(7)	2.42	152	3.54	3.72	10	5.97
	3.17, O(8)	2.29	166							
[DB24C8·**4**][PF$_6$]	3.05, O(2)	2.17	166	3.28, C_C ··· O(6)	2.34	165	3.50	3.75	7	5.89
	3.19, O(8)	2.31	167	3.47, C_D ··· O(4)	2.51	178				
				3.20, C_D ··· O(7)	2.47	134				
[DB24C8·**5**][PF$_6$]	3.10, O(2)	2.23	164	3.33, C_C ··· O(6)	2.45	151	3.63	3.87	13	6.04
	3.08, O(8)	2.24	157	3.47, C_D ··· O(4)	2.49	176				
				3.14, C_D ··· O(7)	2.34	141				
[DB24C8·**6**][PF$_6$]	3.11, O(2)	2.28	152	3.31, C_C ··· O(6)	2.40	158	3.48	3.74	6	5.92
	3.15, O(8)	2.25	179	3.16, C_D ··· O(7)	2.43	133				
[DB24C8·**7**][PF$_6$]	3.09, O(1)	2.38	135	3.32, C_C ··· O(6)	2.52	141	3.55	4.18	13	6.42
	2.93, O(2)	2.07	157	3.23, C_D ··· O(7)	2.40	144				
[DB24C8·**8**][PF$_6$]	3.08, O(2)	2.24	154[c]	3.20, C_D ··· O(7)	2.45	135	3.47	3.73	7	6.05
	3.04, O(3)	2.35	133[c]							
	3.19, O(8)	2.31	165							
[DB24C8·**9**][PF$_6$]	3.10, O(1)	2.37	138	3.28, C_C ··· O(6)	2.50	139	3.59	4.23	15	6.37
	2.93, O(2)	2.09	156	3.23, C_D ··· O(7)	2.38	147				
[DB24C8·**10**][PF$_6$]	3.02, O(2)	2.14	165	3.21, C_D ··· O(7)	2.37	145	3.74	3.91	13	5.87
	3.11, O(8)	2.26	158							
[DB24C8·**11**][PF$_6$]	3.01, O(1)	2.32	133[d]	3.32, C_C ··· O(6)	2.49	145	3.66	3.95	13	6.02
	3.12, O(8)	2.28	157[d]	3.16, C_D ··· O(7)	2.52	157				
	3.02, O(2)	2.20	151[e]							
	3.05, O(3)	2.34	136[e]							
[DB24C8·**13**][PF$_6$]	2.86, O(2)	1.97	171	3.24, C_C ··· O(6)	2.30	167	3.46	3.65	5	5.96
	3.21, O(8)	2.32	169	3.37, C_D ··· O(4)	2.42	168				

[a] All cations have been normalised to a common equivalent 'chirality'. Atom and ring designations correspond to those given in Fig. 3. The N$^+$–H and C–H distances have been normalised to 0.90 and 0.96 Å, respectively. [b] Though this complex crystallises with two independent supermolecules in the asymmetric unit, only one of these adopts a conformation analogous to that seen in the other structures. Consequently, only this supermolecule has been analysed here. [c–e] Bifurcated hydrogen bonds.

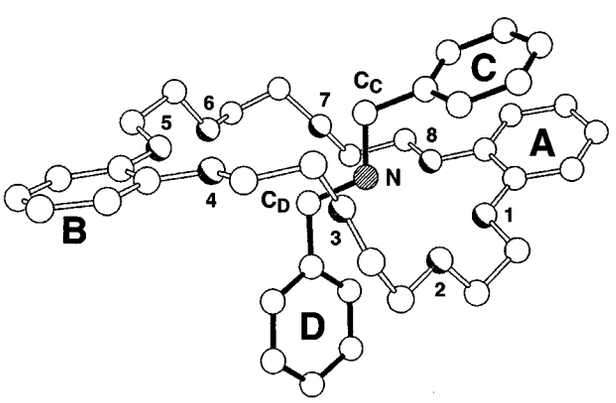

Fig. 3 Crystal structure of one of the two crystallographically-independent [DB24C8·**1**]$^+$ pseudorotaxanes. The aromatic rings' descriptors **A**–**D** are explained in the text.

rotaxanes described in this paper have been elucidated by single crystal X-ray crystallography. As expected, they all possess co-conformations that are very similar, and which are comparable to one of the two independent co-conformations observed[8] for the 1:1 complex formed (Fig. 3) between DB24C8 and the dibenzylammonium cation (**1**$^+$). In all of the crystal structures, the macrocyclic polyether DB24C8 has an extended, approximately C_i-symmetric conformation, with its phenoxyethylene units approximately coplanar with their associated catechol rings, thus maintaining a conformation comparable[16] to that adopted in its uncomplexed state. The different disubstituted dibenzylammonium cations are threaded asymmetrically through the centre of the polyether macroring and have, in each case, one of their aryl rings (**C**) oriented approximately parallel to, and overlaying, one (**A**) of the catechol rings on the DB24C8 macrocycle. The cation's second aryl ring (**D**) is orientated approximately axially with respect to the DB24C8 macrocycle. All of the [2]pseudorotaxanes are stabilised by a combination of [N$^+$–H ··· O] and [C–H ··· O][17] hydrogen bonds, as well as by π–π stacking interactions. Table 4 gives a summary of both the hydrogen bonding and π–π stacking interactions in the 11 complexes studied, together with, for comparison purposes, the data for the 'unsubstituted' complex [DB24C8·**1**]$^+$ that has been reported previously.[8] The identities of the interacting sites, listed in this Table, are identified in Fig. 3, which illustrates the solid state structure of the complex [DB24C8·**1**]$^+$. There is a high degree of consistency in the hydrogen bonding patterns, which appear to be independent of the nature of the substituent present on rings **C** and **D**. The geometries associated with the π–π stacking interactions between rings **A** and **C** are also very similar, the largest deviations being associated with those cations endowed with more sterically demanding substituents, *e.g.* in the [DB24C8·**9**]$^+$ complex. Table 5 summarises the conformational details of the cations in the 12 structures studied. The conformations of the cations are also very similar, their C–CH$_2$–NH$_2^+$–CH$_2$–C backbones adopting a near-planar all-*anti* geometry. Ring **C** is usually inclined fairly steeply to this backbone, tilt angles ranging between 58 and 78° (average 73°), whereas ring **D** has a shallower angle of incline in all of the structures, except in the complex [DB24C8·**13**]$^+$, where the orientation is almost orthogonal.

Although there are no major differences in the crystal structures of the individual [2]pseudorotaxane units, there are marked contrasts in their packing structures. The 1:1 pseudorotaxane complexes [DB24C8·**2**]$^+$, [DB24C8·**4**]$^+$ and [DB24C8·**6**]$^+$ stack to form 'dimer pairs', as illustrated in Fig. 4, with the substituted aryl ring **C** of the cation of one [2]pseudorotaxane unit being π-stacked with its C_i-related counterpart. The mean interplanar separations between the aryl rings **C** of the cations are 3.55, 3.53 and 3.50 Å, respectively, with associated centroid–centroid separations of 4.26, 3.86 and 3.82 Å.

In the [DB24C8·**3**]$^+$ complex, the aryl ring **D** of the cation—

Table 5 Comparison of the cations' torsion angles in their DB24C8 complexes[a]

	C_C–Ar/°[b]	C_C–N/°	N–C_D/°	C_D–Ar/°[b]
[DB24C8·**1**]$^+$[c]	−67	−180	−172	−52
[DB24C8·**2**]$^+$	−75	−175	−173	−40
[DB24C8·**3**]$^+$	−58	−169	−169	−55
[DB24C8·**4**]$^+$	−75	−172	−171	−41
[DB24C8·**5**]$^+$	−75	−175	−176	−42
[DB24C8·**6**]$^+$	−76	−172	−169	−40
[DB24C8·**7**]$^+$	−78	−183	−170	−61
[DB24C8·**8**]$^+$	−73	−170	−170	−44
[DB24C8·**9**]$^+$	−78	−183	−171	−61
[DB24C8·**10**]$^+$	−73	−178	−175	−49
[DB24C8·**11**]$^+$	−71	−176	−171	−58
[DB24C8·**13**]$^+$	−78	−167	−163	−82

[a] All cations have been normalised to a common equivalent 'chirality'. Atom designations correspond to those given in Fig. 3. [b] The out-of-plane tilts of each ring are those looking down the C_C–Ar and C_D–Ar bonds, respectively. [c] Though this complex crystallises with two independent supermolecules in the asymmetric unit, only one of these adopts a conformation analogous to that seen in the other structures. Accordingly, only this supermolecule has been analysed here.

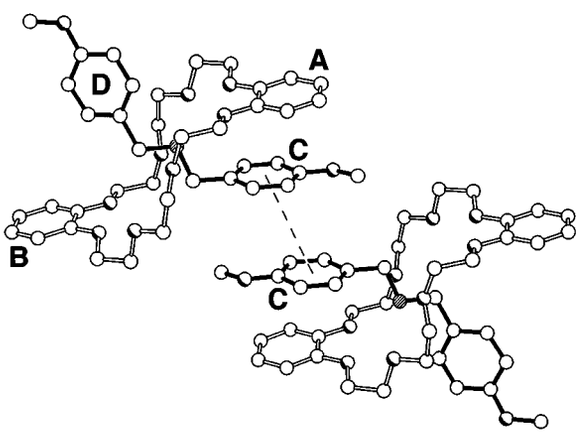

Fig. 4 The 'dimer pair' generated through π–π stacking of the aromatic rings **C** of two units of the pseudorotaxane [DB24C8·**2**]$^+$ in the solid state. Similar packing motifs are observed for the pseudorotaxanes [DB24C8·**4**]$^+$ and [DB24C8·**6**]$^+$.

which is not involved in *intra*pseudorotaxane stacking interactions—in one pseudorotaxane supermolecule is π-stacked with ring **C** of the cation of the next, *via* a glide plane, to produce a pseudopolyrotaxane[18] superstructure (Fig. 5). Rings **C** and **D** of glide-related [2]pseudorotaxane supermolecules are inclined by *ca.* 13° to each other, with centroid–centroid and mean interplanar separations of 4.12 and 3.57 Å, respectively. The angle subtended by the vectors linking the centroids of rings **A** and **C** of one pseudorotaxane and **D** of the next is 152°.

The crystals of the [DB24C8·**5**]$^+$ complex contain two pseudorotaxanes of only one 'chirality'—spontaneous resolution having occurred upon crystallisation. The 1 : 1 complexes pack to give (Fig. 6) helical[4e] pseudopolyrotaxane chains that are held together by edge-to-face interactions[19] between rings **B** and **D**. Ring **B** of one supermolecule is inclined by *ca.* 89° to ring **D** of the next with a centroid–centroid separation of 5.08 Å.

The crystal structure of the [DB24C8·**8**]$^+$ complex reveals that the π-stacked 'dimer pairs', of the type observed for the complexes [DB24C8·**2**]$^+$, [DB24C8·**4**]$^+$ and [DB24C8·**6**]$^+$, extend *via* parallel π-stacking, involving rings **D** of adjacent C_i-related pseudorotaxane supermolecules, to form (Fig. 7) a π-stacked pseudopolyrotaxane supramolecular array. In this case, the centroid–centroid and interplanar separations between rings **D** of adjacent supermolecules are 3.92 and 3.56 Å, respectively, while those between rings **C** are 3.86 and 3.51 Å. Accompanying this extended aryl–aryl stacking mode is a

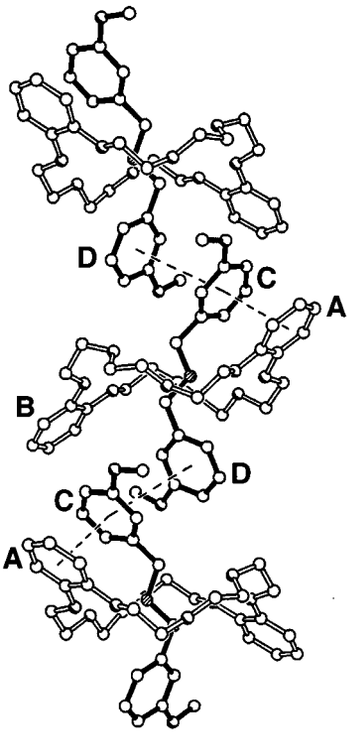

Fig. 5 View of the pseudopolyrotaxane $([DB24C8·\mathbf{3}]^+)_n$ that is generated by means of aryl–aryl stacking interactions in the solid state

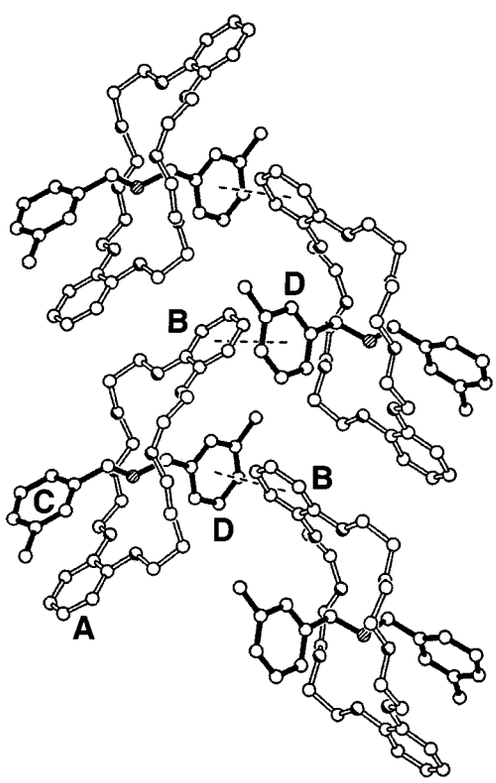

Fig. 6 Portrayal of the helical pseudopolyrotaxane supramolecular array that is produced *via* the noncovalent polymerisation of the pseudorotaxane [DB24C8·**5**]$^+$ in the solid state

short[20] contact (3.26 Å) between the bromine atom attached to ring **D** of one pseudorotaxane and one of the polyether oxygen atoms of an adjacent pseudorotaxane within the same chain.

In the structures of the [DB24C8·**7**]$^+$ and [DB24C8·**9**]$^+$ complexes, there is 'dimer pair' formation analogous to that seen in, for example, the complex [DB24C8·**2**]$^+$ (Fig. 4), but involving (Fig. 8) ring **D** of C_i-related supermolecules (as opposed to ring **C**)—the centroid–centroid and mean interplanar separations

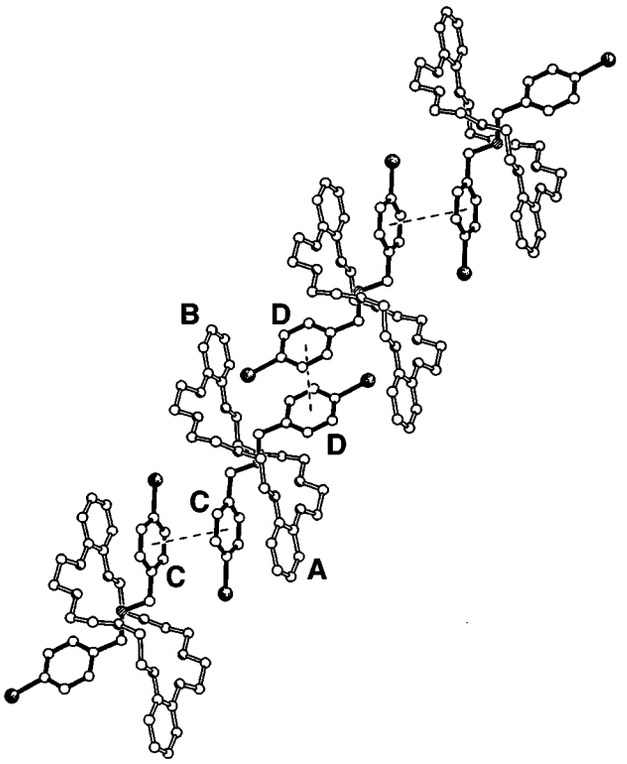

Fig. 7 Pseudopolyrotaxane superarchitecture $([DB24C8\cdot\mathbf{8}]^+)_n$ that is created as a result of π–π and [Br · · · O] interactions in the solid state

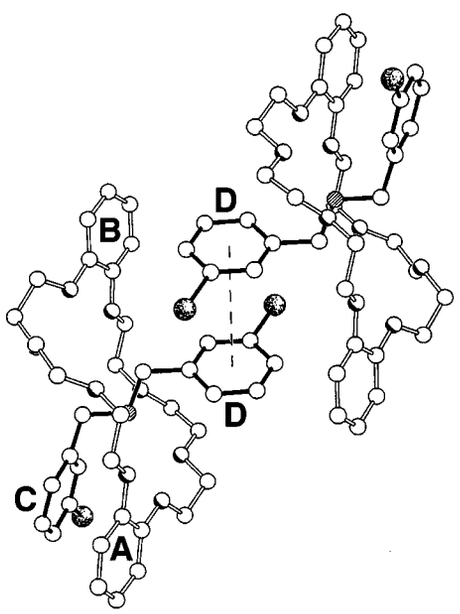

Fig. 8 'Dimer pair' formed by means of π–π stacking interactions between the aromatic rings **D** of two units of the pseudorotaxane $[DB24C8\cdot\mathbf{9}]^+$ in the solid state. A similar packing motif is observed for the pseudorotaxane $[DB24C\mathbf{8}\cdot\mathbf{7}]^+$.

are 3.94 and 3.51 Å for $[DB24C8\cdot\mathbf{7}]^+$ and 4.11 and 3.58 Å for $[DB24C8\cdot\mathbf{9}]^+$, respectively.

The packing motif observed[21] for the $[DB24C8\cdot\mathbf{10}]^+$ complex is identical to that observed for the $[DB24CB\cdot\mathbf{7}]^+$ and $[DB24C8\cdot\mathbf{9}]^+$ complexes, with respective centroid–centroid and interplanar separations of 4.19 and 3.79 Å between rings **D** of C_i-related [2]pseudorotaxanes. This pseudorotaxane dimer is further stabilised (Fig. 9) *via* pairs of [O–H · · · O] hydrogen bonds between the carboxy moiety of one $\mathbf{10}^+$ cation and an oxygen atom—specifically, O(6)—in one of the polyether linkages of the DB24C8 macroring of a symmetry-related

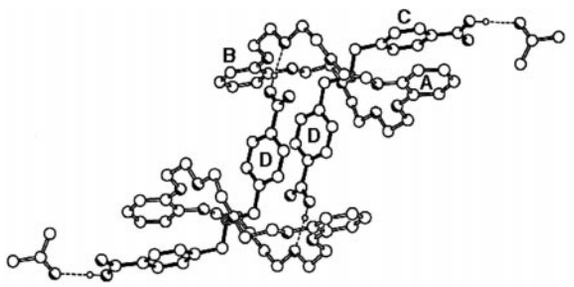

Fig. 9 View of the crystal structure of the $([DB24C8\cdot\mathbf{10}\cdot Me_2CO]^+)_2$ supermolecule

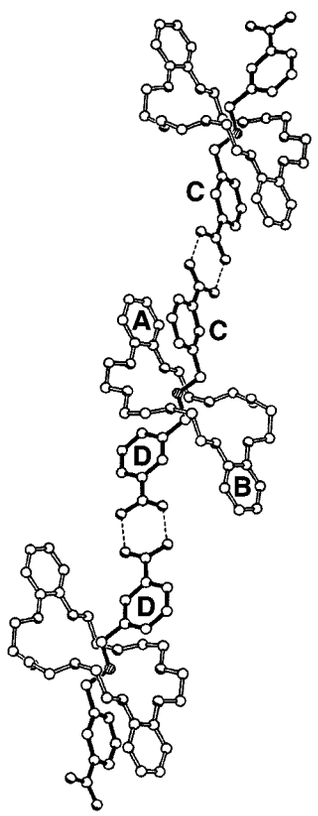

Fig. 10 Pseudopolyrotaxane $([DB24C8\cdot\mathbf{11}]^+)_n$ that is formed by combining two hydrogen bonding motifs—*viz.*, the threading of dibenzylammonium ions through the DB24C8 macroring and the carboxyl dimer—in the solid state

[2]pseudorotaxane and *vice versa*. The respective [O · · · O] and [H · · · O] distances are 2.73 and 1.85 Å, while the [O–H · · · O] angle is 165°. Further propagation of this recognition motif is halted by the intervention of an Me_2CO solvent molecule, which is hydrogen bonded to the vacant carboxy donor site attached to ring **C** of each cation. The associated hydrogen bonding geometries are 2.78, 1.88 Å and 173°, respectively.

Although there were small amounts of Me_2CO solvent in the crystals of $[DB24C8\cdot\mathbf{11}]^+$, they did not interfere with the 'expected' hydrogen bonding pattern—supramolecular polymerisation, employing the conventional hydrogen bonds of the carboxy dimer ([O · · · O] = 2.63 Å) generates[21] the hydrogen bonded pseudopolyrotaxane superstructure illustrated in Fig. 10.

In the final structure examined—*viz.*, $[DB24C8\cdot\mathbf{13}]^+$—spontaneous resolution occurs once again in the crystals and a face-to-face helical[4e] π-stacked pseudopolyrotaxane superstructure is formed, as portrayed in Fig. 11. Rings **C** and **D** of adjacent screw-related cations are inclined by *ca.* 2° with respect to one another and have centroid–centroid and interplanar separations of 3.91 and 3.60 Å, respectively. The angle subtended

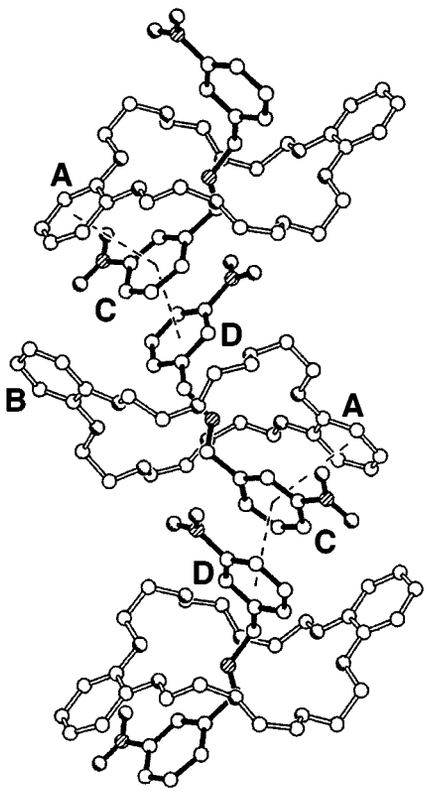

Fig. 11 Helical supramolecular array $([DB24C8\cdot\mathbf{13}]^+)_n$ that is produced *via* the π–π-facilitated noncovalent polymerisation of the pseudorotaxane $[DB24C8\cdot\mathbf{13}]^+$

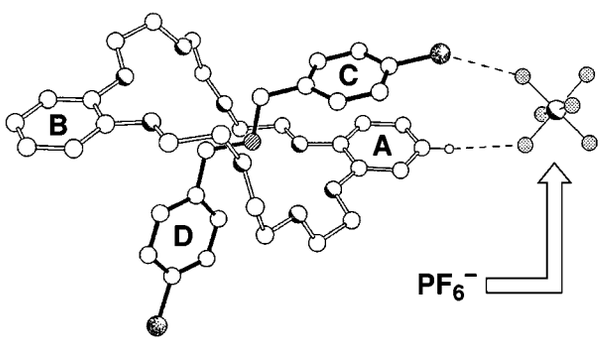

Fig. 12 Solid state association of a PF_6^- anion with the pseudorotaxane $[DB24C8\cdot\mathbf{6}]^+$ *via* [Cl · · · F] and [C–H · · · F] interactions. The pseudorotaxane $[DB24C8\cdot\mathbf{8}]^+$ associates with a PF_6^- anion through a similar recognition motif.

by the vector linking the centres of rings **A**–**C** and **C**–**D** within this chain is 141°.

Other supramolecular features worthy of note are the close approaches involving (Fig. 12) one of the halogen atoms of the [2]pseudorotaxanes $[DB24C8\cdot\mathbf{6}]^+$ and $[DB24C8\cdot\mathbf{8}]^+$ with one of the fluorine atoms of their associated PF_6^- anions.[22] The relevant [Cl · · · F] and [Br · · · F] distances are both 3.22 Å. In both cases, there is a secondary approach of one of the hydrogen atoms—at the 3-position on catechol ring **A**—and one of the anion's other fluorine atoms. The respective [C · · · F]/[H · · · F] distances and [C–H · · · F] angles are 3.54, 2.65 Å and 160° in the pseudorotaxane $[DB24C8\cdot\mathbf{6}]^+$, while they are 3.54, 2.66 Å and 158° in its bromine-containing congener $[DB24C8\cdot\mathbf{8}]^+$.

Conclusions

We have designed, synthesised and evaluated a supramolecular system in which the solution phase binding strengths of pseudorotaxane complexes can be controlled precisely by the judicious manipulation of substituents (Scheme 3). A correlation

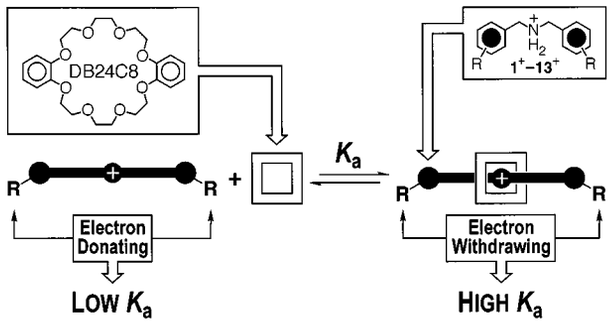

Scheme 3 Schematic diagram illustrating how the stabilities of the DB24C8–dibenzylammonium ion-based pseudorotaxanes are dependent on the nature of the substituent attached to the cations' aromatic rings. Dibenzylammonium ions bearing electron donating groups generate pseudorotaxanes with low stabilities, while those endowed with electron withdrawing substituents form highly stable pseudorotaxanes.

between substitution and activity has been accepted in the context of the covalent bond for decades[13]—the work presented here shows, along with results from other research laboratories,[14] that this phenomenon can be extended to include the realm of the noncovalent bond. Conceptually, supramolecular design is thus evolving one step further so that the strength of complexation, *i.e.* the K_a value, can be 'fine-tuned' in a manner of which an engineer would be proud. We envisage that this kind of 'supramolecular engineering' will form the basis for the fabrication of device-like materials[23]—based upon molecular components—which will surely become a part of everyday life in the new millennium. Nevertheless, such engineering may require the exact positioning of individual device-like (super)-molecules, a feat which we have not, as yet, been able to achieve predictably, in the solid state, with the pseudorotaxanes described in this Keynote Article. Indeed, it seems that, in general,[24] crystallisation processes are difficult to manipulate in a predictable manner as they are kinetically-controlled.[25] In other words, the solid state may be too restrictive for formulating device-like materials from molecular/supramolecular components—the synthetic supramolecular chemist must explore alternative ways of structurally organising and functionally integrating chemical architectures (*e.g.* on surfaces,[26] at air–water interfaces[27] or on the peripheries of dendrimers[28]).

Experimental

Previously published procedures were used to prepare the salts $\mathbf{1}\cdot PF_6$,[8] $\mathbf{10}\cdot PF_6$ and $\mathbf{11}\cdot PF_6$,[21] while the crown ether DB24C8 is commercially available from Aldrich. Anhydrous MeOH and THF were obtained from Aldrich in Sure/Seal containers and were stored under dry N_2. Melting points were determined employing an Electrothermal 9200 melting point apparatus and are uncorrected. Routine ^1H NMR spectra were recorded on either Bruker AC300 or AMX400 spectrometers (at 300.1 or 400.1 MHz, respectively) using the deuterated solvent as the lock and the residual solvent as internal reference. Coupling constants (J) are reported in Hz. Routine ^{13}C NMR spectra were recorded on the Bruker AC300 spectrometer (75.5 MHz) employing the PENDANT pulse sequence. Liquid secondary ion (LSI) mass spectra were obtained from a VG Zabspec mass spectrometer equipped with a caesium ion source and utilising an *m*-nitrobenzyl alcohol matrix. Microanalyses were performed by the University of North London Microanalytical Services.

General Synthetic Procedure A—bis(4-methoxybenzyl)-ammonium hexafluorophosphate $2\cdot PF_6$

A solution of 4-methoxybenzylamine (1.01 g, 7.4 mmol) and 4-anisaldehyde (1.00 g, 7.4 mmol) in PhMe (150 ml) was heated

under reflux with stirring for 24 h—the H_2O produced was collected in a Dean–Stark separator. The solution was filtered while hot and the solvent evaporated off under reduced pressure to furnish 4-methoxybenzylidene-4-methoxybenzylamine[29] (1.79 g, 95%) as a yellow oil [$\delta_H(CDCl_3)$ 3.82 (3H, s), 3.84 (3H, s), 4.77 (2H, s), 6.95 (4H, m), 7.32 (2H, d, *J* 9), 7.77 (2H, d, *J* 9), 8.32 (1H, s)], which was dissolved in a THF–MeOH solution (1 : 1, 100 ml), before being treated with $NaBH_4$ (0.28 g, 7.4 mmol) with stirring at 20 °C. After an additional 2 h, a further portion of $NaBH_4$ (0.28 g, 7.4 mmol) was added to the reaction mixture. Thereupon, the solution was stirred for 16 h, before being treated with 6 M HCl (50 ml). The solvents were evaporated off and the residue was partitioned between 5 M KOH (100 ml) and CH_2Cl_2 (100 ml), the aqueous phase being extracted further with CH_2Cl_2 (3 × 75 ml). The combined organic extracts were washed with H_2O (75 ml), dried ($MgSO_4$), filtered and concentrated to afford bis(4-methoxybenzyl)amine[29] (1.20 g, 60%) as a yellow oil [$\delta_H(CDCl_3)$ 3.74 (4H, s), 3.79 (6H, s), 6.92 (4H, d, *J* 8), 7.29 (4H, d, *J* 8)]. An aliquot of this amine (0.50 g, 1.95 mmol) was dissolved in $CHCl_3$ (10 ml) and HCl gas bubbled through the stirred reaction mixture for 30 min. The chloride salt, that had precipitated out of solution, was collected, washed with Et_2O (10 ml) and dried under high vacuum. The solid was suspended in Me_2CO (90 ml) and then treated with an aqueous NH_4PF_6 solution (0.2 M, 60 ml) to effect dissolution. After stirring for 30 min, the Me_2CO was removed *in vacuo* so that the hexafluorophosphate salt precipitated out of solution. The remainder was treated with H_2O (50 ml) and the residual white solid collected, before being washed with more H_2O (30 ml). Drying provided **2**·PF_6 as a white solid (0.68 g, 87%), mp 126 °C with decomp. (Found: C, 47.8; H, 5.1; N, 3.4. $C_{16}H_{20}F_6NO_2P$ requires C, 47.7; H, 5.0; N, 3.5%); $\delta_H(CD_3CN)$ 3.79 (6H, s), 4.08 (4H, s), 6.92 (4H, d, *J* 8), 7.33 (4H, d, *J* 8); $\delta_C(CD_3CN)$ 51.5, 56.0, 115.2, 123.4, 132.6, 161.5; *m*/*z* 258 $(M - PF_6)^+$.

Bis(3-methoxybenzyl)ammonium hexafluorophosphate 3·PF_6

Using Procedure A, 3-methoxybenzylamine (1.01 g, 7.4 mmol) was condensed with 3-anisaldehyde (1.00 g, 7.4 mmol) to afford 3-methoxybenzylidene-3-methoxybenzylamine (1.80 g, 96%) as a yellow oil [$\delta_H(CDCl_3)$ 3.83 (3H, s), 3.88 (3H, s), 4.84 (2H, s), 6.86–6.91 (1H, m), 6.98–7.10 (1H, m), 7.26–7.49 (6H, m), 8.40 (1H, s)]. The imine was then reduced to afford bis(3-methoxybenzyl)amine (1.50 g, 83%) as a pale yellow oil [$\delta_H(CDCl_3)$ 3.72 (4H, s), 3.79 (6H, s), 6.79 (2H, dd, *J* 9, 1), 6.90–6.96 (4H, m), 7.20–7.28 (2H, m)], the entirety of which was transformed into the white solid **3**·PF_6 (1.80 g, 77%), mp 125 °C with decomp. (Found: C, 47.8; H, 5.0; N, 3.4. $C_{16}H_{20}F_6NO_2P$ requires C, 47.7; H, 5.0; N, 3.5%); $\delta_H(CD_3CN)$ 3.80 (6H, s), 4.18 (4H, s), 6.78–6.94 (6H, m), 7.35–7.39 (2H, m); $\delta_C(CD_3CN)$ 52.2, 55.9, 116.1, 116.3, 123.0, 131.1, 132.6, 160.8; *m*/*z* 258 $(M - PF_6)^+$.

General Synthetic Procedure B—bis(4-methylbenzyl)ammonium hexafluorophosphate 4·PF_6

The Procedure was exactly the same as Procedure A, except that different conditions were utilised for the protonation step. 4-Methylbenzylamine (1.01 g, 8.3 mmol) was condensed with 4-tolualdehyde (1.00 g, 8.3 mmol) to yield 4-methylbenzylidene-4-methylbenzylamine[30] (1.85 g, 100%) as a pale yellow oil [$\delta_H(CDCl_3)$ 2.34 (3H, s), 2.41 (3H, s), 4.78 (2H, s), 7.10–7.30 (6H, m), 7.68 (2H, d, *J* 8), 8.36 (1H, s)]. Reduction provided bis(4-methylbenzyl)amine[30] (1.01 g, 56%) [$\delta_H(CDCl_3)$ 2.43 (6H, s), 3.88 (4H, s), 7.22 (4H, d, *J* 8), 7.33 (4H, d, *J* 8)], which was boiled with 6 M HCl (150 ml) for 24 h with stirring. Upon cooling, the solvent was evaporated off under reduced pressure, then the residual white solid was washed with H_2O (20 ml), Me_2CO (20 ml) and Et_2O (20 ml). Anion exchange yielded the title compound **4**·PF_6 (1.48 g, 92%), mp 205–207 °C with decomp. (Found: C, 51.7; H, 5.4; N, 3.8. $C_{16}H_{20}F_6NP$ requires C, 51.8; H, 5.4; N, 3.8%); $\delta_H(CD_3CN)$ 2.35 (6H, s), 4.15 (4H, s), 7.26 (4H, d, *J* 8), 7.33 (4H, d, *J* 8); $\delta_C(CD_3CN)$ 21.1, 52.0, 128.3, 130.5, 131.0, 140.8; *m*/*z* 226 $(M - PF_6)^+$.

Table 6 Solvent systems employed for the crystallisation of the pseudorotaxanes [DB24C8·**1**][PF_6]–[DB24C8·**11**][PF_6] and [DB24C8·**13**][PF_6] using the liquid diffusion[a] technique

Pseudorotaxane	Solvent	Precipitant
[DB24C8·**1**][PF_6]	$CHCl_3$	*n*-C_6H_{14}
[DB24C8·**2**][PF_6]	CH_2Cl_2	Et_2O
[DB24C8·**3**][PF_6]	MeCN	Pr^i_2O
[DB24C8·**4**][PF_6]	Me_2CO	Et_2O
[DB24C8·**5**][PF_6]	Me_2CO	Pr^i_2O
[DB24C8·**6**][PF_6]	Me_2CO	Pr^i_2O
[DB24C8·**7**][PF_6]	Me_2CO	Pr^i_2O
[DB24C8·**8**][PF_6]	$(ClCH_2)_2$	*n*-C_6H_{14}
[DB24C8·**9**][PF_6]	Me_2CO	Pr^i_2O
[DB24C8·**10**][PF_6]	Me_2CO	Pr^i_2O
[DB24C8·**11**][PF_6]	Me_2CO	Pr^i_2O
[DB24C8·**13**][PF_6]	Me_2CO	Et_2O

[a] Equimolar quantities of the pseudorotaxanes' constituents were dissolved in a small amount of the solvent (in which all species are totally soluble), then the precipitant was layered on top of the resulting solution carefully. X-ray quality crystals were obtained after several days, when the precipitant had diffused into the solution completely.

Bis(3-methylbenzyl)ammonium hexafluorophosphate 5·PF_6

Employing Procedure B, 3-methylbenzylamine (1.01 g, 8.3 mmol) was condensed with 3-tolualdehyde (1.00 g, 8.3 mmol) to furnish 3-methylbenzylidene-3-methylbenzylamine (1.49 g, 80%) as a yellow liquid [$\delta_H(CDCl_3)$ 2.34 (3H, s), 2.36 (3H, s), 4.84 (2H, s), 7.04–7.41 (6H, m), 7.59 (1H, d, *J* 8), 7.69 (1H, s), 8.36 (1H, s)], which was reduced to afford bis(3-methylbenzyl)amine (1.12 g, 75%) as a yellow solid [$\delta_H(CDCl_3)$ 2.45 (6H, s), 3.84 (4H, s), 7.13–7.38 (8H, m)]. An aliquot of this amine (1.00 g, 4.4 mmol) was converted into the title compound **5**·PF_6, which was a white solid (1.23 g, 75%), mp 206 °C with decomp. (Found: C, 51.9; H, 5.3; N, 3.7. $C_{16}H_{20}F_6NP$ requires C, 51.8; H, 5.4; N, 3.8%); $\delta_H(CD_3CN)$ 2.35 (6H, s), 4.14 (4H, s), 7.22–7.35 (8H, m); $\delta_C(CD_3CN)$ 21.3, 52.4, 128.1, 130.0, 131.3, 131.4, 131.7, 140.0; *m*/*z* 226 $(M - PF_6)^+$.

Bis(4-chlorobenzyl)ammonium hexafluorophosphate 6·PF_6

Following Procedure B, 4-chlorobenzylamine (1.01 g, 7.1 mmol) was condensed with 4-chlorobenzaldehyde (1.00 g, 7.1 mmol) to obtain crude 4-chlorobenzylidene-4-chlorobenzylamine[31] as a yellow solid. Recrystallisation from MeOH furnished the pure imine (1.05 g, 56%) as yellow crystals [$\delta_H(CDCl_3)$ 4.76 (2H, s), 7.22–7.35 (4H, m), 7.41 (2H, d, *J* 8), 7.72 (2H, d, *J* 8), 8.32 (1H, s)], which were reduced to yield bis(4-chlorobenzyl)amine[32] (0.71 g, 70%) as a colourless liquid [$\delta_H(CDCl_3)$ 3.75 (4H, s), 7.22–7.37 (8H, m)]. Protonation and anion exchange provided **6**·PF_6 as a white solid (0.83 g, 79%), mp 215 °C with decomp. (Found: C, 41.2; H, 3.9; N, 3.6. $C_{14}H_{14}Cl_2F_6NP$ requires C, 40.8; H, 3.4; N, 3.4%); $\delta_H(CD_3CN)$ 4.15 (4H, s), 7.41–7.53 (8H, m); $\delta_C(CD_3CN)$ 51.5, 129.7, 130.0, 132.9, 136.1; *m*/*z* 266 $(M - PF_6)^+$.

Bis(3-chlorobenzyl)ammonium hexafluorophosphate 7·PF_6

Using Procedure B, 3-chlorobenzylamine (1.01 g, 7.1 mmol) was condensed with 3-chlorobenzaldehyde (1.00 g, 7.1 mmol) to furnish 3-chlorobenzylidene-3-chlorobenzylamine[31] (1.78 g, 95%) as a yellow oil [$\delta_H(CDCl_3)$ 4.79 (2H, s), 7.16–7.57 (6H, m), 7.64 (1H, d, *J* 9), 7.87 (1H, s), 8.33 (1H, s)], which was reduced to afford bis(3-chlorobenzyl)amine[33] (1.60 g, 90%) as a yellow oil [$\delta_H(CDCl_3)$ 3.76 (4H, s), 7.17–7.27 (6H, m), 7.38 (2H, s)]. Treatment with acid followed by counterion exchange gave **7**·PF_6 as a white solid (2.21 g, 89%), mp 199–200 °C with decomp. (Found: C, 40.7; H, 3.5; N, 3.3. $C_{14}H_{14}Cl_2F_6NP$ requires C, 40.8; H, 3.4; N, 3.4%); $\delta_H(CD_3CN)$ 4.19 (4H, s), 7.38–7.51 (8H, m); $\delta_C(CD_3CN)$ 51.7, 129.7, 130.7, 131.1, 131.7, 133.4, 135.1; *m*/*z* 266 $(M - PF_6)^+$.

Table 7 Crystal data, data collection and refinement parameters[a]

Data	[DB24C8·**1**][PF_6]	[DB24C8·**2**][PF_6]	[DB24C8·**3**][PF_6]	[DB24C8·**4**][PF_6]	[DB24C8·**5**][PF_6]	[DB24C8·**6**][PF_6]
Formula	$C_{38}H_{48}NO_8 \cdot PF_6$	$C_{40}H_{52}NO_{10} \cdot PF_6$	$C_{40}H_{52}NO_{10} \cdot PF_6$	$C_{40}H_{52}NO_8 \cdot PF_6$	$C_{40}H_{52}NO_8 \cdot PF_6$	$C_{38}H_{46}NO_8Cl_2 \cdot PF_6$
Solvent	0.25 H_2O	—	—	—	—	—
Formula weight	1592.5	851.8	851.8	819.8	819.8	860.6
Colour, habit	Clear platy needles	Clear prisms	Clear prisms	Clear prisms	Clear prismatic platy needles	Clear prisms
Crystal size/mm	0.73 × 0.33 × 0.10	0.27 × 0.20 × 0.17	1.00 × 0.90 × 0.87	0.80 × 0.77 × 0.73	0.83 × 0.60 × 0.13	1.00 × 0.93 × 0.80
Lattice type	Triclinic	Monoclinic	Monoclinic	Monoclinic	Monoclinic	Monoclinic
Space group symbol, number	$P\bar{1}$, 2	$P2_1/n$, 14	$P2_1/c$, 14	$P2_1/c$, 14	$P2_1$, 4	$P2_1/c$, 14
Cell dimensions						
a/Å	14.430(2)	10.850(2)	15.687(1)	10.644(1)	10.632(1)	10.674(1)
b/Å	15.788(4)	10.788(2)	15.157(1)	35.887(2)	11.423(1)	35.733(2)
c/Å	18.536(5)	36.572(7)	17.980(2)	10.889(1)	17.793(1)	10.798(2)
α/°	73.30(2)	—	—	—	—	—
β/°	75.79(2)	91.45(2)	102.61(1)	90.19(1)	104.36(1)	90.08(1)
γ/°	84.10(2)	—	—	—	—	—
V/Å^3	3939(2)	4280(1)	4171.9(6)	4159.0(4)	2093.4(2)	4118(1)
Z	4[b]	4	4	4	2	4
D_c/g cm^{-3}	1.350	1.322	1.356	1.309	1.301	1.388
F(000)	1674	1792	1792	1728	864	1792
Radiation used	Cu-Kα	Cu-Kα	Cu-Kα	Cu-Kα	Cu-Kα	Cu-Kα
μ/mm^{-1}	1.33	1.28	1.32	1.26	1.25	2.47
θ range/°	1.5–55.0	2.4–60.0	2.9–62.1	2.5–60.0	2.6–62.0	2.5–60.0
No. of unique reflections						
measured	9857	6351	6543	6140	3472	6085
observed, $\|F_o\| > 4\sigma(\|F_o\|)$	6629	4231	4591	4371	2771	3669
Absorption correction	—	—	—	—	—	—
Maximum, minimum transmission	—	—	—	—	—	—
No. of variables	1027	577	556	526	518	530
R_1 (observed data)[c]	0.063	0.057	0.070	0.067	0.060	0.084
wR_2 (observed data)[d]	0.068[e]	0.141[f]	0.176[f]	0.166[f]	0.160[f]	0.201[f]
Weighting factors *a*, *b*[g]	0.0005[h]	0.065, 1.851	0.098, 2.854	0.090, 2.837	0.112, 0.208	0.104, 8.483
Largest difference peak, hole/e Å^{-3}	0.31, −0.25	0.27, −0.20	0.42, −0.38	0.44, −0.34	0.48, −0.25	0.65, −0.56

Bis(4-bromobenzyl)ammonium hexafluorophosphate 8·PF_6

Utilising Procedure B, 4-bromobenzylamine (1.19 g, 6.8 mmol) was condensed with 4-bromobenzaldehyde (1.18 g, 6.8 mmol) to give 4-bromobenzylidene-4-bromobenzylamine (2.20 g, 92%) as a colourless oil [$\delta_H(CDCl_3)$ 4.75 (2H, s), 7.20 (2H, d, *J* 8), 7.47 (2H, d, *J* 8), 7.58 (2H, d, *J* 8), 7.66 (2H, d, *J* 8), 8.31 (1H, s)]. A portion of this imine (2.10 g, 6.0 mmol) was reduced to provide bis(4-bromobenzyl)amine[33] (1.85 g, 90%) as a low melting white solid [$\delta_H(CDCl_3)$ 3.74 (4H, s), 7.22 (4H, d, *J* 8), 7.45 (4H, d, *J* 8)]. An aliquot of this amine (1.81 g, 5.1 mmol) was then converted, using the standard procedures, into the white solid **8**·PF_6 (1.44 g, 57%), mp 220 °C with decomp. (Found: C, 33.5; H, 3.0; N, 2.8. $C_{14}H_{14}Br_2F_6NP$ requires C, 33.6; H, 2.8; N, 2.8%); $\delta_H(CD_3CN)$ 4.16 (4H, s), 7.37 (4H, d, *J* 8), 7.62 (4H, d, *J* 8); $\delta_C(CD_3CN)$ 51.6, 124.4, 130.5, 133.0, 133.1; *m*/*z* 356 $(M - PF_6)^+$.

Bis(3-bromobenzyl)ammonium hexafluorophosphate 9·PF_6

Employing Procedure B, condensation of 3-bromobenzylamine (0.80 g, 4.3 mmol) and 3-bromobenzaldehyde (0.80 g, 4.3 mmol) gave 3-bromobenzylidene-3-bromobenzylamine (1.50 g, 99%) as a yellow oil [$\delta_H(CDCl_3)$ 4.74 (2H, s), 7.25–7.42 (6H, m), 7.52 (2H, s), 8.31 (1H, s)], which was reduced to afford bis(3-bromobenzyl)amine (1.18 g, 78%) as a yellow solid [$\delta_H(CDCl_3)$ 3.77 (4H, s), 7.14–7.52 (6H, m), 7.49 (2H, s)]. This amine was then transformed into the title compound **9**·PF_6, which was a white solid (1.21 g, 73%), mp 222 °C with decomp. (Found: C, 33.3; H, 2.8; N, 2.9. $C_{14}H_{14}Br_2F_6NP$ requires C, 33.6; H, 2.8; N, 2.8%); $\delta_H(CD_3CN)$ 4.17 (4H, s), 7.34–7.47 (4H, m), 7.64–7.72 (4H, m); $\delta_C(CD_3CN)$ 51.6, 123.0, 130.0, 131.8, 132.2, 133.6, 134.0; *m*/*z* 356 $(M - PF_6)^+$.

General Synthetic Procedure C—bis(4-nitrobenzyl)ammonium hexafluorophosphate 12·PF_6

The protocol used was analogous, in every way, to Procedure B except for the reduction step. 4-Nitrobenzylamine (0.94 g, 6.2 mmol) was condensed with 4-nitrobenzaldehyde (0.93 g, 6.2 mmol) to give 4-nitrobenzylidene-4-nitrobenzylamine[34] (1.61 g, 91%) as a yellowish liquid [$\delta_H(CDCl_3)$ 4.95 (2H, s), 7.56 (2H, d, *J* 9), 7.96 (2H, d, *J* 8), 8.23 (2H, d, *J* 9), 8.32 (2H, d, *J* 8), 8.54 (1H, s)]. A portion of this imine (0.60 g, 2.1 mmol) was dissolved in anhydrous THF (13 ml) at 20 °C. HCl gas was bubbled through the stirred reaction mixture, which became hot and began to reflux. The flask was then cooled in an ice bath, and $NaBH_3CN$ (0.10 g, 1.6 mmol), dissolved in anhydrous MeOH (3.7 ml), was added to the reaction mixture in one portion. The whole was then stirred at 20 °C for 1 h, the solvent was removed *in vacuo* and the residue partitioned between 0.1 M NaOH (10 ml) and CH_2Cl_2 (15 ml). The aqueous phase was extracted further with CH_2Cl_2 (3 × 15 ml) and then the combined organic extracts were dried (K_2CO_3), filtered and concentrated to afford crude bis(4-nitrobenzyl)amine[35] as a yellow solid. The pure amine was obtained as dark yellow crystals after recrystallisation from EtOH (0.23 g, 38%) [$\delta_H(CDCl_3)$ 3.96 (4H, s), 7.54 (4H, d, *J* 9), 8.19 (4H, d, *J* 9)]. Standard protonation followed by counterion exchange furnished **12**·PF_6 as a yellow solid (0.30 g, 87%), mp 198 °C with decomp. (Found: C, 38.8; H, 3.3; N, 9.9. $C_{14}H_{14}F_6N_3O_4P$ requires C, 38.8; H, 3.3; N, 9.7%); $\delta_H(CD_3CN)$ 4.32 (4H, s), 7.72 (4H, d, *J* 9), 8.26 (4H, d, *J* 9); $\delta_C(CD_3CN)$ 51.6, 124.9, 132.5, 137.8, 148.1; *m*/*z* 288 $(M - PF_6)^+$.

Bis(3-nitrobenzyl)ammonium hexafluorophosphate 13·PF_6

Using Procedure C, 3-nitrobenzylamine (1.01 g, 6.7 mmol) was condensed with 3-nitrobenzaldehyde (1.01 g, 6.7 mmol) to afford 3-nitrobenzylidene-3-nitrobenzylamine[34] (1.88 g, 98%) as a tan solid [$\delta_H(CDCl_3)$ 4.96 (2H, s), 7.51–7.78 (3H, m), 8.18 (2H, d, *J* 9), 8.22 (1H, s), 8.34 (1H, d, *J* 8), 8.53 (1H, s), 8.64 (1H, s)], which was reduced to produce, after recrystallisation from EtOH, bis(3-nitrobenzyl)amine[35] as yellow crystals (1.30

Table 7 (*Contd.*)

Data	[DB24C8·**7**][PF_6]	[DB24C8·**8**][PF_6]	[DB24C8·**9**][PF_6]	[DB24C8·**10**][PF_6]	[DB24C8·**11**][PF_6]	[DB24C8·**13**][PF_6]
Formula	$C_{38}H_{46}NO_8Cl_2\cdot PF_6$	$C_{38}H_{46}NO_8Br_2\cdot PF_6$	$C_{38}H_{46}NO_8Br_2\cdot PF_6$	$C_{40}H_{48}NO_{12}\cdot PF_6$	$C_{40}H_{48}NO_{12}\cdot PF_6$	$C_{38}H_{46}N_3O_{12}\cdot PF_6$
Solvent	—	—	—	Me_2CO	0.25 Me_2CO	—
Formula weight	860.6	949.6	949.6	937.8	894.3	881.8
Colour, habit	Clear prisms	Clear blocks	Clear prisms	Clear prisms	Clear prismatic needles	Yellow rhombs
Crystal size/mm	1.00 × 0.83 × 0.50	0.50 × 0.40 × 0.33	0.93 × 0.47 × 0.23	0.93 × 0.83 × 0.40	0.50 × 0.30 × 0.13	0.80 × 0.70 × 0.43
Lattice type	Monoclinic	Triclinic	Monoclinic	Triclinic	Triclinic	Orthorhombic
Space group symbol, number	$P2_1/c$, 14	$P\bar{1}$, 2	$P2_1/c$, 14	$P\bar{1}$, 2	$P\bar{1}$, 2	$P2_12_12_1$, 19
Cell dimensions						
a/Å	10.902(1)	10.619(2)	10.839(1)	11.908(1)	11.015(3)	11.687(1)
b/Å	11.052(1)	10.941(2)	11.105(1)	12.336(1)	11.022(1)	16.972(1)
c/Å	34.930(3)	17.869(2)	35.472(2)	16.627(2)	19.764(2)	21.324(1)
α/°	—	94.29(1)	—	79.92(1)	78.39(1)	—
β/°	96.29(1)	91.48(1)	96.50(1)	83.55(1)	77.94(2)	—
γ/°	—	90.05(1)	—	76.17(1)	89.81(1)	—
V/Å^3	4183.5(6)	2069.5(5)	4236.6(4)	2328.8(4)	2296.6(7)	4229.6(5)
Z	4	2	4	2	2	4
D_c/g cm^{-3}	1.366	1.524	1.489	1.337	1.293	1.385
F(000)	1792	968	1936	984	936	1840
Radiation used	Cu-Kα	Mo-Kα	Cu-Kα	Mo-Kα	Cu-Kα	Cu-Kα
μ/mm^{-1}	2.43	2.07	3.45	0.15	1.26	1.37
θ range/°	2.6–60.0	1.9–25.0	2.5–60.0	2.0–25.0	2.3–63.0	3.3–64.0
No. of unique reflections						
measured	6199	7212	6237	8157	7400	3922
observed, $\lvert F_o\rvert > 4\sigma(\lvert F_o\rvert)$	3804	4001	3772	4844	5257	3019
Absorption correction	Semi-empirical	Semi-empirical	Semi-empirical	—	—	—
Maximum, minimum transmission	0.21, 0.08	0.36, 0.30	0.24, 0.11	—	—	—
No. of variables	514	514	514	622	586	550
R_1 (observed data)[c]	0.068	0.058	0.076	0.079	0.083	0.068
wR_2 (observed data)[d]	0.174[f]	0.112[f]	0.198[f]	0.217[f]	0.246[f]	0.186[f]
Weighting factors *a*, *b*[g]	0.094, 2.321	0.043, 1.744	0.125, 2.891	0.126, 1.334	0.170, 0.713	0.120, 1.169
Largest difference peak, hole/e Å^{-3}	0.43, −0.35	0.70, −0.66	0.68, −0.54	0.50, −0.42	0.65, −0.30	0.33, −0.25

[a] Details in common: graphite monochromated radiation, ω-scans, Siemens P4 diffractometer, 293 K. [b] There are two crystallographically independent supermolecules in the asymmetric unit. [c] $R_1 = \Sigma\lvert\lvert F_o\rvert - \lvert F_c\rvert\rvert/\Sigma\lvert F_o\rvert$. [d] $wR_2 = \sqrt{\{\Sigma[w(F_o^2 - F_c^2)^2]/\Sigma[w(F_o^2)^2]\}}$. [e] Refinement based on *F* using observed data. The value given is for R_w. [f] Refinement based on F^2 using all data. [g] $w^{-1} = \sigma^2(F_o^2) + (aP)^2 + bP$. [h] The value given is *g* in $w^{-1} = \sigma^2(F) + gF^2$.

g, 69%) [$\delta_H(CDCl_3)$ 3.92 (4H, s), 7.43–7.51 (2H, t, *J* 9), 7.70 (2H, d, *J* 9), 8.10 (2H, d, *J* 9), 8.21 (2H, s)]. The amine (1.23 g, 4.24 mmol) was then converted, *via* the standard protocol, into the title compound, which was a pure white solid (1.77 g, 91%), mp 221–223 °C (Found: C, 39.0; H, 3.1; N, 9.8. $C_{14}H_{14}F_6N_3O_4P$ requires C, 38.8; H, 3.3; N, 9.7%); $\delta_H(CD_3CN)$ 4.34 (4H, s), 7.66–7.72 (2H, t, *J* 8), 7.85 (2H, d, *J* 8), 8.35 (2H, d, *J* 8), 8.40 (2H, s); $\delta_C(CD_3CN)$ 51.4, 125.5, 126.1, 131.4, 132.9, 137.5, 149.2; *m*/*z* 288 $(M - PF_6)^+$.

Determination of the stability constants (K_a values) and supramolecular reaction constants (ρ values)

1:1 Mixtures of DB24C8 and the relevant salt (7.0×10^{-3} mmol for both components) were dissolved in the appropriate solvent system (0.7 ml) to adjust the concentration of both species to 1×10^{-2} M. The absolute concentrations of the free ([DB24C8] and [Salt]) and complexed ([DB24C8·Salt]) species in solution were obtained[8] from the relative intensities of the ^{1}H NMR signals (400.1 MHz, 31 °C) of each species, along with each component's original (known) concentration. The K_a values were then calculated using the expression K_a = [DB24C8·Salt]/[DB24C8][Salt]. Linear regression analysis of the log[K_a(R)/K_a(H)] and σ data furnished the best fit line with a slope equivalent to ρ.

X-Ray crystallographic analyses

Single crystals of the pseudorotaxanes, that were suitable for X-ray crystallographic analyses, were obtained, utilising (Table 6) the liquid diffusion method,[36] from equimolar solutions of DB24C8 and the appropriate salt. Table 7 provides a summary of the crystal data, data collection and refinement parameters for complexes [DB24C8·**1**][PF_6]–[DB24C8·**11**][PF_6] and [DB24C8·**13**][PF_6]. Structure solution and refinement details for [DB24C8·**1**][PF_6], [DB24C8·**10**][PF_6] and [DB24C8·**11**]-[PF_6] have been published elsewhere,[8a,21] and so will not be repeated here. The rest of the structures were solved by direct methods and were refined by full matrix least-squares based on F^2. In structures [DB24C8·**2**][PF_6]–[DB24C8·**6**][PF_6], disorder was found in part of one of the polyether linkages. In each case, this was resolved into two partial occupancy orientations, the major occupancy portions of which were refined anisotropically—in [DB24C8·**2**][PF_6] the minor occupancy portions were also refined anisotropically, but in the others they were refined isotropically. In [DB24C8·**2**][PF_6] and [DB24C8·**3**][PF_6], the PF_6^- anions were found to be disordered. In each case, this was resolved into two partial occupancy orientations, the major occupancy portions of which were refined anisotropically—in [DB24C8·**3**][PF_6] the minor occupancy atoms were refined isotropically, whereas in [DB24C8·**2**][PF_6] they were refined anisotropically. The remaining non-hydrogen atoms in all of the structures were refined anisotropically. In each structure the C–H hydrogen atoms were placed in calculated positions, assigned isotropic thermal parameters, $U(H) = 1.2U_{eq}(C)$ [$U(H) = 1.5U_{eq}$(C–Me)], and allowed to ride on their parent atoms. The N–H hydrogen atoms in all the structures were located from ΔF maps and refined isotropically subject to a distance constraint. The absolute structures of [DB24C8·**5**]-[PF_6] and [DB24C8·**13**][PF_6] were determined by use of the Flack parameter, which refined to values of 0.07(16) and 0.10(9) respectively. Computations were carried out using the SHELXTL PC program system.[37] The crystallographic data (excluding structure factors) for the structures reported in Table

7 have been deposited with the Cambridge Crystallographic Data Centre and are available on request. Any such request should be accompanied by a full bibliographic citation for this work, together with the reference codes/numbers ZELFOL (for [DB24C8·**1**][PF_6]),[8a] 100/689 (for [DB24C8·**10**][PF_6] and [DB24C8·**11**][PF_6])[21] and 188/135 (for [DB24C8·**2**][PF_6]–[DB24C8·**9**][PF_6] and [DB24C8·**13**][PF_6]). For details of the deposition scheme, see 'Instructions for Authors', *J. Chem. Soc.*, *Perkin Trans. 2*, available *via* the RSC Web page (http://www.rsc.org/authors).

Acknowledgements

This research was supported in the UK by the Engineering and Physical Sciences Research Council.

References

1 'Molecular Meccano', Part 43. For Part 42, see: C. Hamers, F. M. Raymo and J. F. Stoddart, *Eur. J. Org. Chem.*, in the press.
2 (*a*) M. Mascal, *Contemp. Org. Synth.*, 1994, **1**, 31; (*b*) J.-M. Lehn, *Supramolecular Chemistry*, VCH, Weinheim, 1995; (*c*) *Comprehensive Supramolecular Chemistry*, eds. J. L. Atwood, J. E. D. Davies, D. D. MacNicol and F. Vögtle, Pergamon, Oxford, 1996, 11 vols.
3 M. C. T. Fyfe and J. F. Stoddart, *Acc. Chem. Res.*, 1997, **30**, 393.
4 (*a*) W. T. S. Huck, R. Hulst, P. Timmerman, F. C. J. M. van Veggel and D. N. Reinhoudt, *Angew. Chem.*, *Int. Ed. Engl.*, 1997, **36**, 1006; (*b*) B. Hasenkopf, J.-M. Lehn, N. Boumedine, A. Dupont-Gervais, A. Van Dorsselaer, B. Kniesel and D. Fenske, *J. Am. Chem. Soc.*, 1997, **119**, 10 956; (*c*) D. L. Caulder and K. N. Raymond, *Angew. Chem.*, *Int. Ed. Engl.*, 1997, **36**, 1440; (*d*) R. P. Sijbesma, F. H. Beijer, L. Brunsveld, B. J. B. Folmer, J. H. K. K. Hirschberg, R. F. M. Lange and E. W. Meijer, *Science*, 1997, **278**, 1601; (*e*) D. Whang, J. Heo, C.-A. Kim and K. Kim, *Chem. Commun.*, 1997, 2361; (*f*) L. MacGillivray and J. L. Atwood, *Nature*, 1997, **389**, 469.
5 (*a*) D. Philp and J. F. Stoddart, *Angew. Chem.*, *Int. Ed. Engl.*, 1996, **35**, 1154; (*b*) M. M. Conn and J. Rebek, Jr., *Chem. Rev.*, 1997, **97**, 1647; (*c*) B. Linton and A. D. Hamilton, *Chem. Rev.*, 1997, **97**, 1669; (*d*) R. E. Gillard, F. M. Raymo and J. F. Stoddart, *Chem. Eur. J.*, 1997, **3**, 1933.
6 (*a*) C. J. Pedersen, *J. Am. Chem. Soc.*, 1967, **89**, 7017; (*b*) C. J. Pedersen, *Angew. Chem.*, *Int. Ed. Engl.*, 1988, **27**, 1021.
7 I. Goldberg, in *Inclusion Compounds*, eds. J. L. Atwood, J. E. D. Davies and D. D. MacNicol, Academic Press, London, 1984, vol. 2, pp. 261–335.
8 (*a*) P. R. Ashton, P. J. Campbell, E. J. T. Chrystal, P. T. Glink, S. Menzer, D. Philp, N. Spencer, J. F. Stoddart, P. A. Tasker and D. J. Williams, *Angew. Chem.*, *Int. Ed. Engl.*, 1995, **34**, 1865; (*b*) P. R. Ashton, E. J. T. Chrystal, P. T. Glink, S. Menzer, C. Schiavo, N. Spencer, J. F. Stoddart, P. A. Tasker, A. J. P. White and D. J. Williams, *Chem. Eur. J.*, 1996, **2**, 709; (*c*) P. T. Glink, C. Schiavo, J. F. Stoddart and D. J. Williams, *Chem. Commun.*, 1996, 1483.
9 (*a*) D. B. Amabilino, P.-L. Anelli, P. R. Ashton, G. R. Brown, E. Córdova, L. A. Godínez, W. Hayes, A. E. Kaifer, D. Philp, A. M. Z. Slawin, N. Spencer, J. F. Stoddart, M. S. Tolley and D. J. Williams, *J. Am. Chem. Soc.*, 1995, **117**, 11 142; (*b*) P. R. Ashton, S. J. Langford, N. Spencer, J. F. Stoddart, A. J. P. White and D. J. Williams, *Chem. Commun.*, 1996, 1387; (*c*) H. Sleiman, P. N. W. Baxter, J.-M. Lehn, K. Airola and K. Rissanen, *Inorg. Chem.*, 1997, **36**, 4734; (*d*) A. Mirzoian and A. E. Kaifer, *Chem. Eur. J.*, 1997, **3**, 1052.
10 C. A. Hunter, *Chem. Soc. Rev.*, 1994, **23**, 101.
11 M. C. T. Fyfe and J. F. Stoddart, *Adv. Supramol. Chem.*, in the press and references cited therein.
12 For a review dealing with the application of LFERs to supramolecular chemistry, see: H.-J. Schneider, *Chem. Soc. Rev.*, 1994, **23**, 227.
13 (*a*) L. P. Hammett and H. L. Pfluger, *J. Am. Chem. Soc.*, 1933, **55**, 4079; (*b*) L. P. Hammett, *J. Chem. Educ.*, 1966, **43**, 464; (*c*) C. Hansch, A. Leo and R. W. Taft, *Chem. Rev.*, 1991, **91**, 165; (*d*) C. Hansch, *Acc. Chem. Res.*, 1993, **26**, 147.
14 For some other examples of Hammett correlations 'beyond the molecule', *i.e.*, involving supramolecular chemistry, see: (*a*) R. Ungaro, B. El Haj and J. Smid, *J. Am. Chem. Soc.*, 1976, **98**, 5198; (*b*) Y. Hashida and K. Matsui, *Bull. Chem. Soc. Jpn.*, 1980, **53**, 551; (*c*) R. M. Izatt, J. D. Lamb, C. S. Swain, J. J. Christensen and B. L. Haymore, *J. Am. Chem. Soc.*, 1980, **102**, 3032; (*d*) F. Cozzi, M. Cinquini, R. Annunziata, T. Dwyer and J. S. Siegel, *J. Am. Chem. Soc.*, 1992, **114**, 5729; (*e*) M. S. Islam, R. A. Pethrick, D. Pugh and M. J. Wilson, *J. Chem. Soc.*, *Faraday Trans.*, 1997, **93**, 387; (*f*) J. N. H. Reek, A. H. Priem, H. Engelkamp, A. E. Rowan, J. A. A. W. Elemans and R. J. M. Nolte, *J. Am. Chem. Soc.*, 1997, **119**, 9956.
15 For leading references on this method, see: J. C. Adrian, Jr. and C. S. Wilcox, *J. Am. Chem. Soc.*, 1991, **113**, 678.
16 I. R. Hanson, D. L. Hughes and M. R. Truter, *J. Chem. Soc.*, *Perkin Trans. 2*, 1976, 972.
17 T. Steiner, *Chem. Commun.*, 1997, 727.
18 M. C. T. Fyfe and J. F. Stoddart, *Coord. Chem. Rev.*, in the press.
19 (*a*) M. Nishio, Y. Umezawa, M. Hirota and Y. Takeuchi, *Tetrahedron*, 1995, **51**, 8865; (*b*) M. Nishio, M. Hirota and Y. Umezawa, *The CH/π Interaction*, Wiley-VCH, New York, 1998.
20 F. H. Allen, J. P. M. Lommerse, V. J. Hoy, J. A. K. Howard and G. R. Desiraju, *Acta Crystallogr.*, *Sect. B*, 1997, **53**, 1006.
21 P. R. Ashton, M. C. T. Fyfe, S. K. Hickingbottom, S. Menzer, J. F. Stoddart, A. J. P. White and D. J. Williams, *Chem. Eur. J.*, 1998, **4**, 577.
22 (*a*) W. Zhang, C. Bensimon and R. J. Crutchley, *Inorg. Chem.*, 1993, **32**, 5808; (*b*) J. Powell, M. J. Horvath and A. Lough, *J. Chem. Soc.*, *Dalton Trans.*, 1996, 1669.
23 (*a*) A. P. de Silva, H. Q. Gunaratne, T. Gunnlaugsson, A. J. M. Huxley, C. P. McCoy, J. T. Rademacher and T. E. Rice, *Chem. Rev.*, 1997, **97**, 1515; (*b*) V. Balzani, M. Gómez-López and J. F. Stoddart, *Acc. Chem. Res.*, 1998, **31**, 405.
24 For exceptions, see: G. R. Desiraju, *Chem. Commun.*, 1997, 1475 and references cited therein.
25 A. Gavezzotti, *Acc. Chem. Res.*, 1994, **27**, 309.
26 P. Laitenberger, C. G. Claessens, F. M. Kuipers, F. M. Raymo, R. E. Palmer and J. F. Stoddart, *Chem. Phys. Lett.*, 1997, **279**, 209.
27 R. C. Ahuja, P.-L. Caruso, D. Möbius, D. Philp, J. A. Preece, H. Ringsdorf, J. F. Stoddart and G. Wildburg, *Thin Solid Films*, 1996, **285**, 671.
28 T. Dünnwald, R. Jäger and F. Vögtle, *Chem. Eur. J.*, 1997, **3**, 2043.
29 B. R. Henke, A. J. Kouklis and C. H. Heathcock, *J. Org. Chem.*, 1992, **57**, 7056.
30 R. Juday and H. Adkins, *J. Am. Chem. Soc.*, 1955, **77**, 4559.
31 L. Castedo, R. Riguera and M. J. Rodríguez, *Tetrahedron*, 1982, **38**, 1569.
32 A. R. Katzritzky, X. Zhao and G. J. Hitchings, *Synthesis*, 1991, 703.
33 J. von Braun, M. Kühn and J. Weismantel, *Liebigs Ann. Chem.*, 1926, **449**, 249.
34 C. K. Ingold and H. A. Piggott, *J. Chem. Soc.*, 1922, **121**, 2793.
35 E. L. Holmes and C. K. Ingold, *J. Chem. Soc.*, 1925, **127**, 1800.
36 P. G. Jones, *Chem. Br.*, 1981, **17**, 222.
37 SHELXTL PC Version 5.03, Siemens Analytical X-Ray Instruments, Inc., Madison, WI, 1994.

Paper 8/02406E
Received 30*th March* 1998
Accepted 27*th May* 1998